

Statistical properties of intensity of partially polarised semiconductor laser light backscattered by a single-mode optical fibre

A.E. Alekseev, B.G. Gorshkov, V.T. Potapov

Abstract. We report the results of studying statistical properties of the intensity of partially polarised coherent light backscattered by a single mode optical fibre. An expression is derived for the deviation of the backscattered light intensity depending on the scattering region length, the degree of the light source coherence and the degree of scattered light polarisation. It is shown that the backscattered light in a fibre scattered-light interferometer is partially polarised with the polarisation degree $P = 1/3$ in the case of external perturbations of the interferometer fibre.

Keywords: backscattered light, fibre scattered-light interferometer, depolarisation.

1. Introduction

Studying the properties of coherent light backscattered by a single-mode fibre is of great interest for the rapidly developing coherent fibre reflectometry. Optimisation of the backscattered signal parameters can improve such reflectometer characteristics as reflected waveform contrast and reflectometer sensitivity to external perturbations, which is important for fabricating distributed phase-sensitive sensors with improved characteristics [1, 2]. The backscattered light parameters are analysed in this paper using a fibre scattered-light interferometer (FSLI), in which there occurs a multipath interference of the fields backscattered by an optical fibre medium. In the simplest case, the FSLI is a segment of a single-mode optical fibre, which backscatters coherent optical radiation. All interfering fields at the FSLI output have random amplitude and phase, and therefore such an interferometer can only be considered statistically. A FSLI is an object with essentially random characteristics, which are random both in time and upon the transition from one implementation of a statistical distribution

of the scattering coefficients $\{\rho\} = \{\rho_1 \rho_2 \dots \rho_n\}$ to another, where ρ_n is the complex amplitude scattering coefficient of any centre corresponding to a fraction of the radiation scattered by the centre and captured by fibre in the opposite direction.

The temporal characteristics of a FSLI are characterised by temporal average values hereinafter denoted by $E_T\langle\dots\rangle$, and the statistical characteristics – by statistical average values hereinafter denoted by $E_\rho\langle\dots\rangle$. The temporal averaging $E_T\langle\dots\rangle$ is related to the scattered light intensity detected by a photodetector and to the noise spectrum intensity that is independently determined for each specific implementation of the distribution coefficients of scattering of centres in the FSLI medium $\{\rho\}$. In changing the implementation of this distribution (for example, when considering another statistically equivalent scattering region), both time-averaged characteristics change randomly; however, for these changes one can introduce such statistical parameters as density distribution and ensemble-averaged distribution of scattering coefficients of the centres $E_\rho\langle\dots\rangle$. The temporal characteristics of the scattered light are determined by the properties of the light source, and the statistical characteristics – by the properties of a scattering medium. Hence we assume below that these two averagings (temporal and statistical) can be carried out independently of each other.

In previous studies we considered statistical properties of the intensity of completely polarised fibre-backscattered coherent radiation [3, 4] and the spectral characteristics of scattered light [5], as well as analysed the feasibility of using an optical fibre segment for recording acoustic effects with the possibility of recovering the waveform of external phase effects [6]. This paper presents the results of studies of statistical properties of intensity of partially polarised backscattered radiation of a FSLI with semiconductor laser sources with varying degrees of coherence, operating in continuous (unmodulated) mode; expressions are derived for the average intensity and its deviation, which determines the contrast of the FSLI interference pattern.

2. Intensity of partially polarised backscattered light

The basic FSLI configuration, which allows the main properties to be analysed, is a FSLI with a scattering segment, shown schematically in Fig. 1. A typical interferogram at the FSLI output is presented in Fig. 2. As a model of a scattering FSLI medium we use a long fibre of length L with evenly distributed scattering centres, i.e., microscopic inhomogeneities of the refractive index [3–7]. At the input of the scattering fibre there occurs multipath interference of the fields of radiation scattered by a large number of centres of the medium in ques-

A.E. Alekseev V.A. Kotelnikov Institute of Radio Engineering and Electronics, Fryazino Branch, Russian Academy of Sciences, pl. Vvedenskogo 1, 114190 Fryazino, Moscow region, Russia; OOO ‘Petrofaiber’, Klinskii proezd 7, 301664 Novomoskovsk, Tula region, Russia; e-mail: aleksey.e.alekseev@gmail.com;

B.G. Gorshkov OOO ‘Petrofaiber’, Klinskii proezd 7, 301664 Novomoskovsk, Tula region, Russia; A.M. Prokhorov General Physics Institute, Russian Academy of Sciences, ul. Vavilova 38, 119991 Moscow, Russia;

V.T. Potapov V.A. Kotelnikov Institute of Radio Engineering and Electronics, Fryazino Branch, Russian Academy of Sciences, pl. Vvedenskogo 1, 114190 Fryazino, Moscow region, Russia; e-mail: v_potapov38@mail.ru

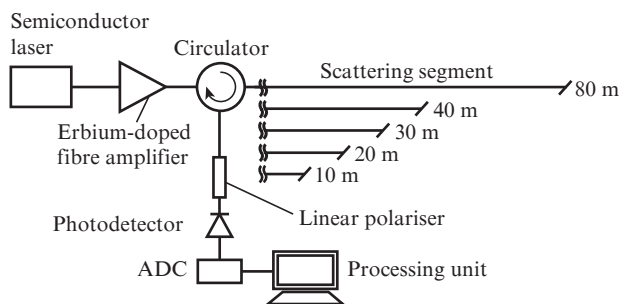


Figure 1. Scheme of the experimental setup.

tion. As noted in papers [3, 7–9], the process of multipath interference of the scattered light fields is similar to the process of formation of a speckle pattern when a rough surface is illuminated by laser radiation. Therefore, to describe the interference of scattered radiation one can use the methods developed in the speckle theory [10–12].

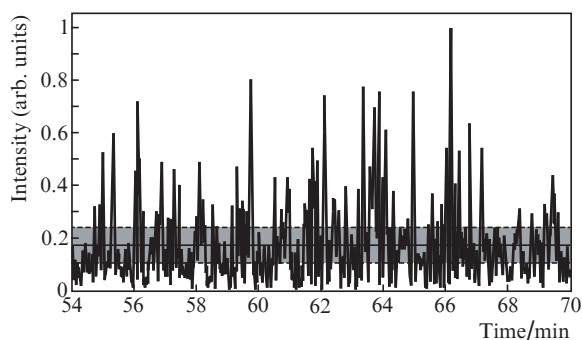


Figure 2. Experimental FSLI interferogram. The continuous horizontal line shows the average value of the intensity, the shaded area – the standard deviation.

By simulating a scattering medium, we assume that the complex amplitude scattering coefficient ρ is a circular complex Gaussian random variable with zero mean [3, 4, 7–12]. This means that its real and imaginary parts ($\text{Re}\rho$ and $\text{Im}\rho$) have a Gaussian distribution over the ensemble, the deviation of the real and imaginary parts being equal. Physically, this assumption is equivalent to the fact that during scattering the complex amplitude of the field source is multiplied by the random variables with Gaussian distributions of the real and imaginary parts with zero mean. We also assume that the complex amplitude scattering coefficients of the different scattering centres are statistically uncorrelated with each other. Mathematically the lack of correlation of the complex scattering coefficients of centres with longitudinal coordinates z_m and z_n , as well as equality of deviations of their real and imaginary parts can be written in the form of two expressions [10]:

$$E_\rho \langle \rho(z_n) \rho(z_m) \rangle = 0, \quad (1)$$

$$E_\rho \langle \rho^*(z_n) \rho(z_m) \rangle = \rho_0 \delta(z_n - z_m), \quad (2)$$

where $E_\rho \langle \dots \rangle$ is the averaging over an ensemble of independent distributions of the scattering coefficients of centres $\{\rho\}$

(or averaging over an ensemble of independent scattering segments); z_n and z_m are the coordinates of the scattering centres located on the axis of the fibre; $\rho_0/2$ is the deviation over an the ensemble of the real and imaginary parts of the scattering coefficients ρ ; and δ is the delta function.

The light source is assumed to be quasi-monochromatic, whose autocorrelation function of the complex field amplitude $A_s(t)$ is [3, 4]

$$E_T \langle A_s(t + \tau) A_s^*(t) \rangle = I_s \exp\left(-\frac{|\tau|}{\tau_{\text{coh}}}\right), \quad (3)$$

where I_s is the intensity of the light source, and τ_{coh} is the coherence time of the source field.

The main characteristic of the optical radiation that can be measured directly in the experiment using the photodetector is its intensity. In scattering continuous-wave (unmodulated) laser radiation by a fibre medium, the scattered light intensity, as described above, depends on the specific implementation of the distribution of the scattering coefficients of centres $\{\rho\}$. At a constant implementation, the scattered light intensity is constant, while at a varying implementation, it changes randomly. Consequently, for the radiation scattered by a random medium of the optical fibre we can introduce the parameter $I_{\text{scat}}^{\text{mean}}$ – the average intensity over the ensemble of independent distributions of the scattering coefficients of centres $\{\rho\}$ or over the ensemble of independent statistically equivalent scattering segments.

During its propagation in the fibre, the polarisation state of radiation continuously changes in a random manner. This change occurs as a result of random birefringence in optical fibre and redistribution of energy of polarisation modes due to random rotation of the birefringence axes – coupling of polarisation modes [13–16]. Depending on the ratio of the parameters (degree of the source coherence, length of the scattering segment, birefringence of the segment and characteristic length of coupling of polarisation modes), the state and degree of polarisation of radiation propagating through fibre change. Isotropic optical fibre is usually modelled by a cascade of successive segments, each of which has random birefringence and random orientation of the birefringence axes [13, 14]. In this case, when the number of independent segments tends to infinity, the radiation occupying the scattering segment becomes completely depolarised in the sense that along the entire length of optical fibre it can have any polarisation state with equal probability.

A change in the statistical distribution of the scattering centres $\{\rho\}$ in time, such as mechanical or thermal perturbation of the scattering segment, leads to the fact that birefringence and orientation of the axes of each segment will vary randomly. As a result, each point of the fibre, the state of radiation polarisation at the output of each segment will also change randomly over time, i.e., the radiation will be depolarised on average over time; in this case, the fibre segment will act like as Billings' depolariser of monochromatic radiation [17, 18]. The Stokes vector of this depolarised light can take any values on the Poincare sphere.

Figure 3a shows the results of simulation of the evolution of the polarisation state of monochromatic radiation at some point of optical fibre at its external perturbation which causes a change in birefringence and orientation of the axes of each of the segments. The radiation is completely depolarised, and its Stokes vector uniformly covers the Poincare sphere. During scattering the polarisation state is assumed unchanged.

Completely depolarised, time-averaged radiation after scattering and propagation in the backward direction partially restores the degree of polarisation so that at the input of the scattering segment, it coincides with the initial polarisation state of radiation coupled into the fibre up to the direction of rotation of the electric vector; the degree of polarisation in the mentioned limit becomes equal to $1/3$ [13–15].

Thus, if the linearly polarised radiation is coupled into a scattering fibre segment exposed external perturbations, the polarisation state of the scattered light will coincide with the polarisation state of the coupled radiation; if the circularly polarised radiation is coupled into the scattering segment, the polarisation state of the scattered light will be orthogonal to the polarisation state of the coupled radiation. In both cases the degree of polarisation is equal to $1/3$. Figure 3b shows the results of modelling the evolution of the polarisation state of monochromatic light scattered at some point in fibre exposed to external perturbations. It can be seen that the distribution of the Stokes vector of the scattered radiation on the Poincare sphere is not uniform and its maximum is located near a point corresponding to the Stokes vector of the initial state of polarisation, which in this case is linear. This behaviour of the backscattered radiation can be explained as follows [13]: during the propagation of radiation in the forward direction, the fibre segment can be modelled by a cascade of segments with uncorrelated Jones matrices that vary randomly at the external perturbation of the fibre. As a result, the radiation at some point of fibre becomes completely depolarised on average over time. During the propagation of light to the point of scattering and back, it passes through the same fibre segment twice, the depolarisation being partially compensated for. Partial restoration of polarisation can also be explained by the following example: if the linearly polarised radiation is coupled into optical fibre, then in the case when at the scattering point the polarisation of light that has reached that point is also linear, the scattered radiation that has returned to the beginning of fibre will have the same linear polarisation as the radiation coupled into the fibre; this follows directly from the analysis using the formalism of Jones matrices and vectors. If at the scattering point the polarised radiation is circular, the scattered radiation returning to the beginning of fibre will have linear polarisation that is orthogonal to polarisation of the coupled radiation [16].

The first event has a much higher probability than the second one, because linear polarisation is represented by the equator on the Poincare sphere, and circular polarisation – by

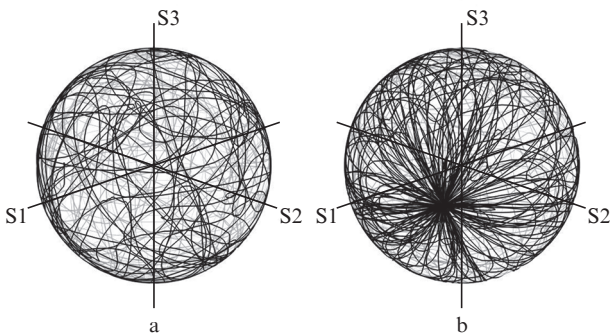


Figure 3. Results of modelling the evolution of the polarisation state of monochromatic light on the Poincare sphere in the case of external perturbations of the fibre (a) for complete temporal depolarisation of radiation ($P = 0$) at the scattering point and (b) partial polarisation ($P = 1/3$) of the scattered light at the beginning of the fibre segment.

its poles, and so the scattered light is more likely to have a polarisation state which is equivalent to the linear polarisation of the coupled radiation. Note an important fact that by depolarisation in this paper is meant depolarisation caused only by the influence of random birefringence in fibre, depolarisation due to the finite width of the spectral characteristic of radiation being neglected because of its ‘narrowness’ [15].

Let denote the degree of polarisation of scattered light by P . The Hermitian matrix of the coherence of partially polarised quasi-monochromatic light can be diagonalized by means of a unitary transformation [11, 19]. As a result, in the new basis the partially polarised monochromatic light of intensity $|A|^2$ can be represented as the sum of two uncorrelated radiations polarised orthogonally in the sense of orthogonality of their Jones vectors. The intensities of each of the two orthogonal polarisation components thus have the forms $|A|^2(1 - P)/2$ and $|A|^2(1 + P)/2$ [11].

The vector of the complex field amplitude of the radiation incident on a scattering centre, which is located at a distance z from the fibre end, can be written as [3, 7]

$$A_{\text{inc}}(t, z) = P(z) A_s(t - z/v_{\text{gr}}) \exp(-\alpha z/2) \exp(-ikz), \quad (4)$$

where $P(z)$ is the Jones matrix describing the change in the polarisation state of light propagating along the fibre axis z ; $A_s(t)$ is the vector of the complex field amplitude of the source; α is the linear attenuation coefficient of the radiation power in fibre; $k = \omega_0/c$ is the constant of radiation propagation; and v_{gr} is the group velocity of light. The complex amplitude of the light field at the beginning of the fibre, scattered by a centre which is located at a distance z from the fibre end, can be written as

$$A_{\text{scat}}(t, z) = M(z) A_s(t - 2z/v_{\text{gr}}) \exp(-\alpha z) \exp(-2ikz) \rho(z), \quad (5)$$

where $M(z) = P(z)^T P(z)$ is the Jones matrix describing the change in the polarisation state of light as it propagates to the point with the coordinate z and back. The total field of the light scattered by the fibre and coming to a photodetector at an instant of time t is

$$A_{\text{scat}}^\rho(t) = \int_0^L M(z) A_s(t - 2z/v_{\text{gr}}) \exp(-\alpha z) \exp(-2ikz) \rho(z) dz. \quad (6)$$

Here, the superscript ρ indicates that the total field is calculated for any specific implementation of the distribution of the scattering coefficients of centres $\{\rho\}$. The total intensity of the scattered light is equal to the time-averaged value of the square of its complex amplitude: $(I_{\text{scat}}^\rho)_{\text{partpol}} = E_T \langle A_{\text{scat}}^\rho(t)^+ A_{\text{scat}}^\rho(t) \rangle$, where the sign ‘+’ denotes the Hermitian conjugation. Considering the scattered light to be partially polarised, and neglecting the attenuation of the radiation power in fibre, we can write the total intensity of the scattered light for a specific implementation of the distribution $\{\rho\}$ as a sum of two uncorrelated intensities:

$$\begin{aligned} (I_{\text{scat}}^\rho)_{\text{partpol}} = & \frac{1-P}{2} \int_0^L \int_0^L E_T \langle A_s^*(t - 2z_1/v_{\text{gr}}) A_s(t - 2z_2/v_{\text{gr}}) \rangle \\ & \times \exp(2ikz_1) \exp(-2ikz_2) \rho^*(z_1) \rho(z_2) dz_1 dz_2 + \\ & + \frac{1+P}{2} \int_0^L \int_0^L E_T \langle A_s^*(t - 2z_1/v_{\text{gr}}) A_s(t - 2z_2/v_{\text{gr}}) \rangle \\ & \times \exp(2ikz_1) \exp(-2ikz_2) \rho^*(z_1) \rho(z_2) dz_1 dz_2. \end{aligned} \quad (7)$$

In averaging over the ensemble $\{\rho\}$, with allowance for (2) and (3), we obtain

$$I_{\text{scat}}^{\text{mean}} = I_s \int_0^L \left(\frac{1-P}{2} + \frac{1+P}{2} \right) \rho_0 dz_2 = I_s L \rho_0 = I_s \frac{v_{\text{gr}}}{2} \rho_0 T. \quad (8)$$

Thus, the average value of the scattered light intensity is independent of the degree of depolarisation and the degree of coherence of the laser source, but is determined only by the length of the scattering segment and the intensity of the light coupled into fibre. The average value of the intensity of the interferogram is shown in Fig. 2 by the horizontal line.

3. Deviation of intensity of partially polarised backscattered light

Another important characteristic of scattered light is the deviation of the scattered light intensity over an ensemble of independent distributions of the scattering coefficients of centres $\{\rho\}$ or over an ensemble of independent scattering segments. This parameter characterises the deviation of the random values of the scattered light intensity from the ensemble-averaged value (8) during the transition from one implementation of the distribution $\{\rho\}$ to another. The contrast of the coherent reflectometer signal or the visibility of the interference pattern for the FSLI can be attributed to the intensity deviation.

The deviation of the scattered light intensity over the ensemble $\{\rho\}$ is defined as a statistical average over the ensemble of the products of intensities for different implementations $\{\rho\}$ minus the square of the average intensity value (8), i.e.,

$$\begin{aligned} D(I_{\text{scat}}) &= E_{\rho} \langle E_T \langle (I_{\text{scat}}^{\rho_1}(t))_{\text{inst}} \rangle E_T \langle (I_{\text{scat}}^{\rho_2}(t))_{\text{inst}} \rangle \rangle - (I_{\text{scat}}^{\text{mean}})^2 \\ &= E_{\rho} \langle I_{\text{scat}}^{\rho_1} I_{\text{scat}}^{\rho_2} \rangle - (I_{\text{scat}}^{\text{mean}})^2, \end{aligned} \quad (9)$$

where ρ_1 and ρ_2 are different implementations of the distribution of the scattering coefficients of centres $\{\rho\}$. Taking into account (7) and the lack of correlation of the fields and intensities of two orthogonal polarisations, for the second moment of a random intensity values over the ensemble $\{\rho\}$ we obtain

$$\begin{aligned} E_{\rho} \langle (I_{\text{scat}}^{\rho_1})_{\text{partpol}} (I_{\text{scat}}^{\rho_2})_{\text{partpol}} \rangle &= \left(\frac{1-P}{2} \right)^2 E_{\rho} \langle I_{\text{scat}}^{\rho_1} I_{\text{scat}}^{\rho_2} \rangle \\ &+ \left(\frac{1+P}{2} \right)^2 E_{\rho} \langle I_{\text{scat}}^{\rho_1} I_{\text{scat}}^{\rho_2} \rangle + 2 \left(\frac{1-P^2}{4} \right) (I_{\text{scat}}^{\text{mean}})^2 \\ &= \frac{1+P^2}{2} E_{\rho} \langle I_{\text{scat}}^{\rho_1} I_{\text{scat}}^{\rho_2} \rangle + \frac{1-P^2}{2} (I_{\text{scat}}^{\text{mean}})^2, \end{aligned} \quad (10)$$

where

$$\begin{aligned} E_{\rho} \langle I_{\text{scat}}^{\rho_1} I_{\text{scat}}^{\rho_2} \rangle &= E_{\rho} \left\langle \int_0^L \int_0^L E_T \left\langle A_s^* \left(t - \frac{2z_1}{v_{\text{gr}}} \right) A_s \left(t - \frac{2z_2}{v_{\text{gr}}} \right) \right\rangle \right. \\ &\times \exp(2ikz_1 - 2ikz_2) \rho^*(z_1) \rho(z_2) dz_1 dz_2 \times \\ &\times \int_0^L \int_0^L E_T \left\langle A_s^* \left(t - \frac{2z_3}{v_{\text{gr}}} \right) A_s \left(t - \frac{2z_4}{v_{\text{gr}}} \right) \right\rangle \\ &\times \exp(2ikz_3 - 2ikz_4) \rho^*(z_3) \rho(z_4) dz_3 dz_4 \left. \right\rangle. \end{aligned} \quad (11)$$

Since the amplitudes of the scattering coefficients of centres for each specific implementation of the distribution $\{\rho\}$ and the complex field amplitudes are statistically independent of each other, their average can be carried out independently [7]. Expression (11) is transformed to the form:

$$\begin{aligned} E_{\rho} \langle I_{\text{scat}}^{\rho_1} I_{\text{scat}}^{\rho_2} \rangle &= \int_0^L \int_0^L \int_0^L \int_0^L \left[E_T \left\langle A_s^* \left(t - \frac{2z_1}{v_{\text{gr}}} \right) A_s \left(t - \frac{2z_2}{v_{\text{gr}}} \right) \right\rangle \right. \\ &\times \exp(2ikz_1 - 2ikz_2) E_T \left\langle A_s^* \left(t - \frac{2z_3}{v_{\text{gr}}} \right) A_s \left(t - \frac{2z_4}{v_{\text{gr}}} \right) \right\rangle \\ &\times \exp(2ikz_3 - 2ikz_4) \left. \right] E_{\rho} \langle \rho^*(z_1) \rho(z_2) \rho^*(z_3) \rho(z_4) \rangle \\ &\times dz_1 dz_2 dz_3 dz_4. \end{aligned} \quad (12)$$

We use below the Gaussian moment theorem for complex random variables that are presumably the complex scattering coefficients ρ [20]:

$$\begin{aligned} E_{\rho} \langle \rho_{i1}^* \rho_{i2}^* \dots \rho_{iN}^* \rho_{j1} \rho_{j2} \dots \rho_{jM} \rangle &= \begin{cases} 0 & N \neq M, \\ \sum_{i,j=1}^{N,M} E_{\rho} \langle \rho_{i1}^* \rho_{j1} \rangle E_{\rho} \langle \rho_{i2}^* \rho_{j2} \rangle \dots E_{\rho} \langle \rho_{iN}^* \rho_{jM} \rangle, & N = M. \end{cases} \end{aligned} \quad (13)$$

Then, taking (2) into account we obtain

$$\begin{aligned} E_{\rho} \langle \rho^*(z_1) \rho(z_2) \rho^*(z_3) \rho(z_4) \rangle &= E_{\rho} \langle \rho^*(z_1) \rho(z_2) \rangle E_{\rho} \langle \rho^*(z_3) \rho(z_4) \rangle \\ &+ E_{\rho} \langle \rho(z_2) \rho^*(z_3) \rangle E_{\rho} \langle \rho^*(z_1) \rho(z_4) \rangle \\ &= \rho_0^2 \delta(z_1 - z_2) \delta(z_3 - z_4) + \rho_0^2 \delta(z_2 - z_3) \delta(z_1 - z_4). \end{aligned} \quad (14)$$

In view of (14) the expression for the second moment (12) takes the form

$$\begin{aligned} E_{\rho} \langle I_{\text{scat}}^{\rho_1} I_{\text{scat}}^{\rho_2} \rangle &= \rho_0^2 \int_0^L \int_0^L \left| A_s \left(t - \frac{2z_1}{v_{\text{gr}}} \right) \right|^2 \left| A_s \left(t - \frac{2z_2}{v_{\text{gr}}} \right) \right|^2 \\ &\times dz_1 dz_2 + \rho_0^2 \int_0^L \int_0^L E_T \left\langle A_s^* \left(t - \frac{2z_1}{v_{\text{gr}}} \right) A_s \left(t - \frac{2z_2}{v_{\text{gr}}} \right) \right\rangle \\ &\times E_T \left\langle A_s^* \left(t - \frac{2z_2}{v_{\text{gr}}} \right) A_s \left(t - \frac{2z_1}{v_{\text{gr}}} \right) \right\rangle dz_1 dz_2. \end{aligned} \quad (15)$$

Now using (3), we obtain

$$\begin{aligned} E_{\rho} \langle I_{\text{scat}}^{\rho_1} I_{\text{scat}}^{\rho_2} \rangle &= \rho_0^2 \int_0^L \int_0^L I_s^2 dz_1 dz_2 \\ &+ \rho_0^2 \int_0^L \int_0^L \exp \left(-\frac{4|z_2 - z_1|}{v_{\text{gr}} \tau_{\text{coh}}} \right) dz_1 dz_2. \end{aligned} \quad (16)$$

By changing the variables, $\tau_1 = 2z_1/v_{\text{gr}}$, $\tau_2 = 2z_2/v_{\text{gr}}$, $T = 2L/v_{\text{gr}}$, we obtain a more convenient equation:

$$\begin{aligned} E_{\rho} \langle I_{\text{scat}}^{\rho_1} I_{\text{scat}}^{\rho_2} \rangle &= \frac{v_{\text{gr}}^2}{4} \rho_0^2 \int_0^T \int_0^T I_s^2 d\tau_1 d\tau_2 \\ &+ \frac{v_{\text{gr}}^2}{4} \rho_0^2 \int_0^T \int_0^T I_s^2 \exp \left(-\frac{2|\tau_2 - \tau_1|}{\tau_{\text{coh}}} \right) d\tau_1 d\tau_2. \end{aligned} \quad (17)$$

The expression for the second central moment, i.e., deviation, with (8) and (10) taken into account takes the form:

$$D(I_{\text{scat}}) = \frac{1+P^2}{2} E_{\rho} \langle I_{\text{scat}}^{\rho_1} I_{\text{scat}}^{\rho_2} \rangle + \frac{1-P^2}{2} (I_{\text{scat}}^{\text{mean}})^2 - (I_{\text{scat}}^{\text{mean}})^2$$

$$= \frac{1+P^2}{2} \frac{v_{\text{gr}}^2}{4\rho_0^2} \int_0^T \int_0^T I_s^2 \exp\left(-\frac{2|\tau_2 - \tau_1|}{\tau_{\text{coh}}}\right) d\tau_1 d\tau_2. \quad (18)$$

After calculating the integral in (18) we obtain the final expression for the deviation of the intensity of partially polarised scattered light:

$$D(I_{\text{scat}}) = \frac{(I_{\text{scat}}^{\text{mean}})^2}{T^2} \frac{1+P^2}{2} \left[\frac{\tau_{\text{coh}}^2}{2} \exp\left(-\frac{2T}{\tau_{\text{coh}}}\right) - \frac{\tau_{\text{coh}}^2}{2} + T\tau_{\text{coh}} \right]. \quad (19)$$

It is important to note that the deviation of intensity is already dependent on the degree of coherence of the source. The standard deviation of the interferogram intensity is shown in Fig. 2 (shaded area). To display the graphic dependence of deviation (19), it is convenient to consider the contrast of the interference pattern. By analogy with [10], as a contrast of the FSLI interferogram we will use the ratio of the intensity standard deviation to its average value over the ensemble $\{\rho\}$:

$$C = \frac{\sqrt{D(I_{\text{scat}})}}{I_{\text{scat}}^{\text{mean}}} = \frac{\tau_{\text{coh}}}{T} \left(\frac{1+P^2}{2} \right)^{1/2} \left[\frac{1}{2} \exp\left(-\frac{2T}{\tau_{\text{coh}}}\right) + \frac{T}{\tau_{\text{coh}}} - \frac{1}{2} \right]^{1/2}. \quad (20)$$

Graphic dependences of contrasts for completely and partially polarised scattered light with the degree of polarisation $P = 1/3$ with reducing degree of coherence of the radiation source are shown in Fig. 4. It is seen that by decreasing the degree of coherence of the radiation source or by increasing the length of the scattering segment of the FSLI the contrast decreases monotonically from a maximum value to zero.

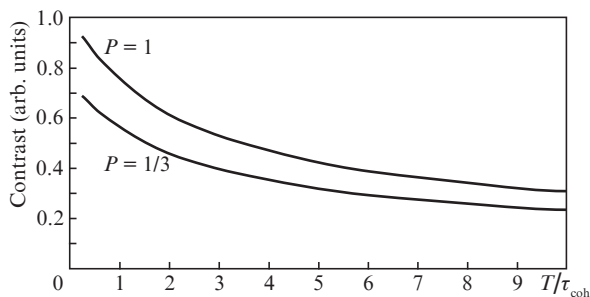


Figure 4. Theoretical dependences of the contrasts of the FSLI interferograms on the ratio of the maximum delay of the interferometer radiation to the coherence time T/τ_{coh} and at varying degrees of polarisation of the scattered light P .

4. Experimental study of the deviation of partially polarised backscattered light intensity

The scheme of the experimental setup for studying the statistical characteristics of the backscattered light intensity is shown in Fig. 1. The 1555-nm radiation with a narrow spectral line width from a distributed-feedback semiconductor laser is amplified by an erbium-doped fibre amplifier to 25 dBm and then coupled through a circulator into a segment of a single-mode isotropic SMF-28 fibre, which is a sensitive element of

the FSLI. We investigated FSLIs with the scattering fibre lengths of 80, 40, 30, 20 and 10 m. The optical fibre of the interferometer scatters light in the opposite direction; the scattered light is coupled output through the circulator and arrives at the photodetector with an RF bandwidth of 10 MHz. Between the circulator and the photodetector we can mount an optical polariser.

To ensure independent statistical distributions of the scattering coefficients, as well as to depolarise the propagating radiation, the fibre is subjected to mechanical and thermal perturbations. We used two types of laser sources: RIO's highly coherent semiconductor laser with the width of the spectral band $\Delta\nu = 2$ kHz and a standard telecom laser diode with the width of the spectral band $\Delta\nu = 480$ kHz.

Figure 5 shows the experimental dependences of the contrast for a laser with high ($\Delta\nu = 2$ kHz) and low ($\Delta\nu = 480$ kHz) degrees of coherence on the length of the scattering segments and degrees of polarisation of the scattered light received by a photodetector. The theoretical dependences are shown by continuous lines.

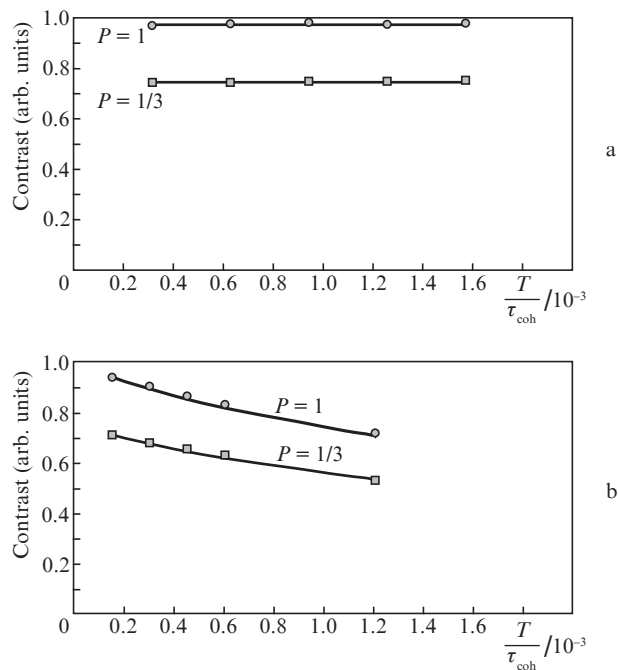


Figure 5. Experimental dependences of the contrast of the FSLI interferogram for a laser with (a) high and (b) low degrees of coherence on the length of the scattering segment (10–80 m) and the degree of polarisation of the scattered light; (a) the contrast of the interferogram does not change, and (b) the contrast of the interferogram decreases.

It follows from Fig. 5a that for a highly coherent laser source, the contrast of the interference pattern for the scattered light with two different degrees of polarisation virtually does not change with increasing length of the scattering segment from 10 to 80 m, i.e., it does not depend on the length of the scattering segment. Figure 5b shows that for a low-coherent laser source, under similar conditions the contrast of the interference pattern decreases, i.e., it depends on the length of the scattering segment. The experimental dependences of the contrast for the sources with varying degrees of coherence and polarisation of the scattered radiation are completely consistent with the theoretical predictions (Fig. 4).

The coincidence of theoretical and experimental curves obtained without the use of an optical polariser gives reason to believe that the degree of polarisation of scattered light is close to $P = 1/3$ [13, 14, 16], which is the result of complete temporal depolarisation of initially completely polarised radiation coupled into the optical fibre of the FSLI. Temporal depolarisation of the radiation introduced into fibre was due to an external perturbation by mechanical or thermal influences. The results of the experiment shows that a simple way to increase the contrast of the interference pattern at the output of a scattering FSLI segment is to use a linear polariser. For a more efficient use of the scattered light power one can use a polarisation coupler that combines two orthogonally aligned linear polarisers; in this case, there is of course a need for an additional optical receiver.

Note that in a coherent reflectometer with a source having a high degree of coherence (the length of the source coherence being an order of the probe pulse duration), the temporal depolarisation is apparently absent, because the reflectometer fibre is not subjected to an external influence (except the point of exposure). Radiation in the probe pulse of the reflectometer in the case of a laser source with a high degree of coherence will be completely polarised, and therefore the scattered light in each time channel will also be completely polarised.

Thus, the experimental dependences of the contrast of the interference pattern of the interferometer match the theoretical dependences with good accuracy. The coincidence of the theoretical results with the experimental ones gives reason to believe that the initial assumptions concerning the properties of the scattered radiation are correct, and the proposed model correctly describes the statistical properties of the scattered light intensity.

5. Conclusions

We have analysed theoretically and experimentally the main statistical characteristics of intensity at the output of a fibre scattered-light interferometer. We have considered the dependences of the average light intensity at the FSLI output and the deviation of this intensity over the ensemble of independent distributions of the scattering centres $\{\rho\}$ on the ratio of the length of the FSLI scattering segment and the degree of coherence of the radiation used, as well as on the degree of polarisation of the scattered radiation. We have shown that the light scattered at the FSLI output, when the fibre is subjected to external perturbations, is partially polarised with the degree of polarisation $P = 1/3$. The use of a linear polariser for the output radiation of the FSLI can increase the interferogram contrast.

References

1. Gorshkov B.G., Paramonov V.M., Kurkov A.S., Kulakov A.T., Zazirnyi M.V. *Kvantovaya Elektron.*, **36** (10), 963 (2006) [*Quantum Electron.*, **36** (10), 963 (2006)].
2. Vdovenko V.S., Gorshkov B.G., et al. *Kvantovaya Elektron.*, **41** (2), 176 (2011) [*Quantum Electron.*, **41** (2), 176 (2011)].
3. Alekseev A.E., Tezadov Ya.A., Potapov V.T. *Radiotekh. Elektron.*, **56** (12), 1522 (2011).
4. Alekseev A.E., Tezadov Ya.A., Potapov V.T. *Kvantovaya Elektron.*, **42** (1), 76 (2012) [*Quantum Electron.*, **42** (1), 76 (2012)].
5. Alekseev A.E., Potapov V.T. *Kvantovaya Elektron.*, **43** (10), 968 (2013) [*Quantum Electron.*, **43** (10), 968 (2013)].
6. Alekseev A.E., Tezadov Ya.A., Potapov V.T. *Pis'ma Zh. Tekh. Fiz.*, **38** (24), 67 (2012).
7. Gysel P., Staubli R.K. *J. Lightwave Technol.*, **8** (4), 561 (1990).

8. Healey P. *Electron. Lett.*, **20** (1), 30 (1984).
9. Healey P. *Electron. Lett.*, **21** (6), 226 (1985).
10. Goodman J.W. *Statistical Properties of Laser Speckle Patterns in Laser Speckle and Related Phenomena*. Ed. by J.C. Dainty (Berlin: Springer-Verlag, 1975).
11. Goodman J.W. *Statistical Optics* (New York: Wiley, 1985; Moscow: Mir, 1988).
12. Goodman J.W. *Speckle Phenomena in Optics: Theory and Applications* (Englewood, Colo.: Roberts & Co, 2007).
13. Corsi F., Galtarossa A., Palmieri L. *J. Lightwave Technol.*, **16** (10), 1832 (1998).
14. Corsi F., Galtarossa A., Palmieri L. *J. Opt. Soc. Am.*, **16** (3), 574 (1999).
15. Huttner B., Gisin B., Gisin N. *J. Lightwave Technol.*, **17** (10), 1843 (1999).
16. van Deventer M.O.J. *Lightwave Technol.*, **11** (12), 1895 (1993).
17. Billings B.H. *J. Opt. Soc. Am.*, **41** (12), 966 (1951).
18. Alekseev E.I., Bazarov E.N. *Pis'ma Zh. Tekh. Fiz.*, **23** (14), 56 (1997).
19. Azzam R.M.A, Bashara N.M. *Ellipsometry and Polarized Light* (Amsterdam: North-Holland Publ., 1977; Moscow: Mir, 1981).
20. Mandel L., Wolf E. *Optical Coherence and Quantum Optics* (Cambridge: Cambridge University Press, 1995; Moscow: Nauka, 2000).